

## Hysteretic behavior in three-dimensional soap film rearrangements

N. Vandewalle,<sup>1</sup> M. Noirhomme,<sup>1</sup> J. Schockmel,<sup>1</sup> E. Mersch,<sup>1</sup> G. Lumay,<sup>1,2</sup> D. Terwagne,<sup>1</sup> and S. Dorbolo<sup>1,2</sup>

<sup>1</sup>*GRASP, Physics Department, University of Liège, B-4000 Liège, Belgium*

<sup>2</sup>*F.R.S.-FRNS, B-1000 Bruxelles, Belgium*

(Received 20 December 2010; published 28 February 2011)

We report experiments on soap film configurations in a triangular prism for which the shape factor can be changed continuously. Two stable configurations can be observed for a range of the shape factor  $h$ , being the prism-height/edge-length ratio. A hysteretic behavior is found, due to the occurrence of another local minima in the free energy. Contrary to a common belief, soap films can be trapped in a particular configuration being different from a global surface minimization. This metastability can be evidenced from a geometrical model based on idealized structures. Depending on the configuration, the transition is either first or second order, providing clues on the structural relaxations taking place into three-dimensional foams, such as T1 rearrangements.

DOI: [10.1103/PhysRevE.83.021403](https://doi.org/10.1103/PhysRevE.83.021403)

PACS number(s): 82.70.Rr, 05.45.-a, 47.20.Dr

### I. INTRODUCTION

A soap film contained by any fixed boundaries is assumed to acquire its minimum free energy when it reaches equilibrium. Since the free energy of a soap film is proportional to its area, this latter is therefore minimized. As a consequence, soap films can be used to solve mathematical problems requiring the minimization of a surface area contained by a complex boundary. Plateau [1] discovered experimentally, over a hundred years ago, that three-dimensional (3D) soap films contained by a framework always satisfy three geometrical conditions:

(i) Three flat soap films intersect along a line. The latter is called a Plateau border.

(ii) The angle between two intersecting surfaces at any point along the Plateau border is  $120^\circ$ .

(iii) Four Plateau borders, each formed by the intersection of three surfaces, meet at a vertex (a node) and the angle between any pair of adjacent Plateau borders is about  $109.4^\circ$ .

Plateau's rules [1,2] are verified for thin films only. When the liquid content increases in the system, the liquid tends to accumulate in the nodes and in the Plateau borders such that various angles different from  $120^\circ$  and  $109.4^\circ$  are observed. For example, it has been checked that when the liquid content is high, a node with a large number of Plateau borders (like eightfold vertex) can be encountered [3].

Three decades ago, Lovett [4] proposed a strong analogy between framework shapes and the distortion of a crystal lattice, suggesting the occurrence of a first order phase transition in soap film arrangements. One of the systems discussed by Lovett is the triangular prism. In such a 3D framework, two different configurations of thin films can be observed. The so-called  $I_{\text{curved}}$  and II configurations are illustrated in Fig. 1, while closeup pictures of the vertices are shown in Fig. 2. When the height  $H$  of the prism is small compared to the edge  $A$  of the triangle, configuration  $I_{\text{curved}}$  is encountered. This configuration is characterized by a horizontal and flat triangular film in the center of the prism with curved (catenoidal) sides, clearly observed in Fig. 2 (top). The other films are six trapezia and three triangles. Some edges are curved in order to satisfy Plateau's rules at the intersection of the films. When the shape of the prism is modified such that the

height  $H$  is high compared to edge length  $A$ , configuration II is observed. In such a soap film arrangement, thin films meet in a vertical Plateau border at the center of the prism. Only two nodes are present at the extremities of this vertical Plateau border. All films remain flat since configuration II is a double tetrahedra structure for which angles satisfy Plateau's rules. By decreasing continuously the ratio  $H/A = h$ , one expects a topological transition between both configurations: The vertical Plateau border becomes a flat face. Indeed, one expects that when decreasing  $h$ , both tetrahedra of configuration II meet forming an unstable sixfold vertex at the center of the prism. The topological rearrangement taking place in the prism is close to a T1 "neighbor switching" event occurring in 2D foams. It has been recently coined "T3" in [5].

Recent studies [6,7] using the Surface Evolver algorithm [8] demonstrated that configurations  $I_{\text{curved}}$  and II could coexist in a small interval of  $h$  values. Figure 3 presents the dimensionless surface area  $s = S/A^2$  of both configurations as a function of the dimensionless shape parameter  $h$ . Each configuration is limited by some instability point: when the horizontal triangular face disappears in configuration  $I_{\text{curved}}$  ( $h \approx 0.49$ ) and when two vertices meet in configuration II ( $h = 1/\sqrt{6} \approx 0.41$ ). The first critical value is obtained numerically with Surface Evolver. The instability was coined "pre-emptive" since the surface area of the horizontal film is not zero at the critical  $h$  value. The second critical value is obtained from a geometrical analysis considering the meeting of tetrahedra centroids. Between  $h \approx 0.41$  and  $h \approx 0.49$ , the coexistence of both configurations is a surprise since the area minimization is often thought to lead thin films toward a unique configuration. The slight difference in surface area indicates that configuration II should be more stable than the  $I_{\text{curved}}$  one. However, experiments conducted only at  $h = 0.5$  [6] proved that one configuration can be changed in the other one by blowing air on the nodes. The transition between  $I_{\text{curved}}$  and II was, however, not eluded because the occurrence of an energy barrier for nonequilibrium situations cannot be explored with Surface Evolver.

In the present paper, we report experimental investigations of the soap film configurations in a triangular prism whose shape can be continuously tuned. The aim of the paper is to show that the system can be trapped in a local minimum

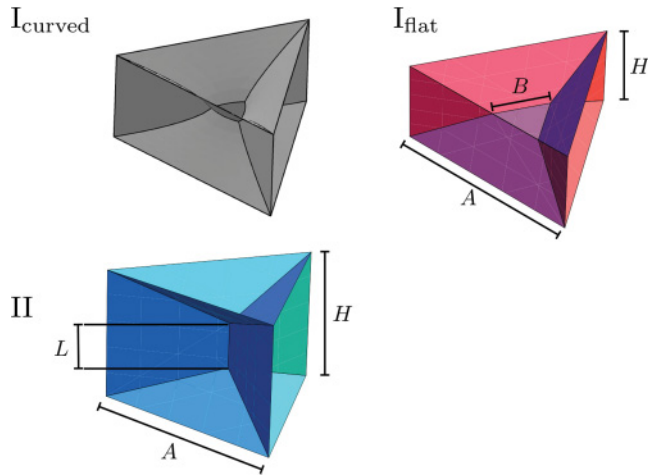


FIG. 1. (Color online) Three soap film configurations are considered in the present paper. Characteristic lengths  $A$ ,  $H$ ,  $L$ , and  $B$  are denoted. Configuration  $I_{\text{curved}}$  with curved edges is observed for small  $h = H/A$  ratios. In order to perform calculations on the latter structure, we consider a similar structure, called  $I_{\text{flat}}$ , with flat surfaces only. The double tetrahedra configuration  $II$  is observed when the ratio  $h$  is high.

of the free energy, leading to hysteretic loops when the geometrical parameters of the soap films are changed. This result provides an additional perspective for the “pre-emptive” instability. Moreover, we propose a geometrical model in order to capture the physics of this phenomenon by tracking the system trajectories along nonequilibrium situations.

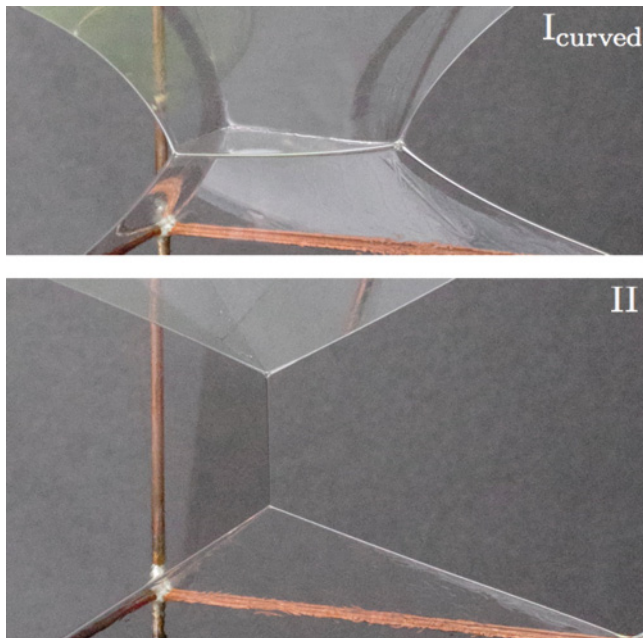


FIG. 2. (Color online) Pictures of the soap film configurations studied in this paper. The closeup near vertices reveal the curvature of the  $I_{\text{curved}}$  configuration (top) while the soap films remain flat for configuration  $II$  (bottom).

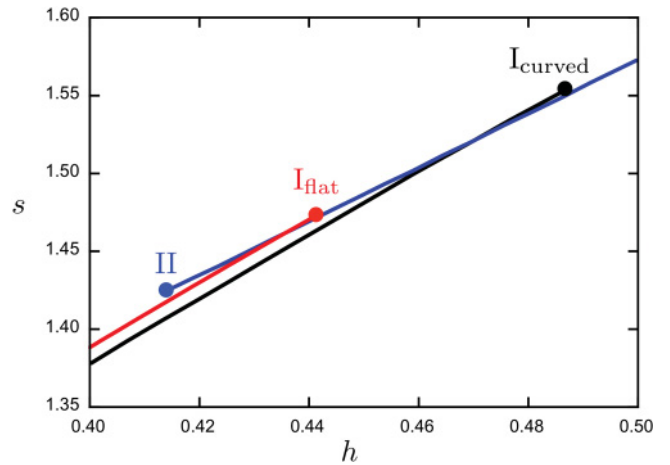


FIG. 3. (Color online) The total surface area  $s = S/A^2$  of soap films in the triangular prism as given by the Surface Evolver algorithm (data adapted from [6]). Both configurations  $I_{\text{curved}}$  and  $II$  are represented. The coexistence of both configurations is possible for  $0.41 \lesssim h \lesssim 0.49$ . Dots corresponds to instability points. The data for  $I_{\text{flat}}$  are also given.

## II. EXPERIMENTS

In order to study soap films, we have built a triangular framework that can be adjusted as depicted in Fig. 4. The framework consists of three vertical rigid wires attached to a horizontal and regular triangle. The edge is kept constant at  $A = 100$  mm but the height  $H$  of the prism can be changed. Indeed, the upper part of the prism is mobile. The diameter of the wires is 1 mm. As illustrated in Fig. 5, the prism is first immersed into a soap and water mixture and thereafter placed near a graduated vertical line for measurements. Measurements start 30 sec after soap film creation in order to allow

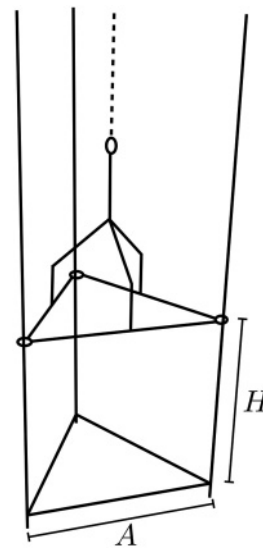


FIG. 4. Illustration of the triangular framework used for the experiments with relevant parameters. The framework consists of three vertical rigid wires attached to a horizontal and regular triangle. The length of a triangular edge is  $A = 10$  cm. A mobile triangle, parallel to the former, can be placed at different vertical positions  $H$  along the vertical framework by using a thin wire (dashed line).

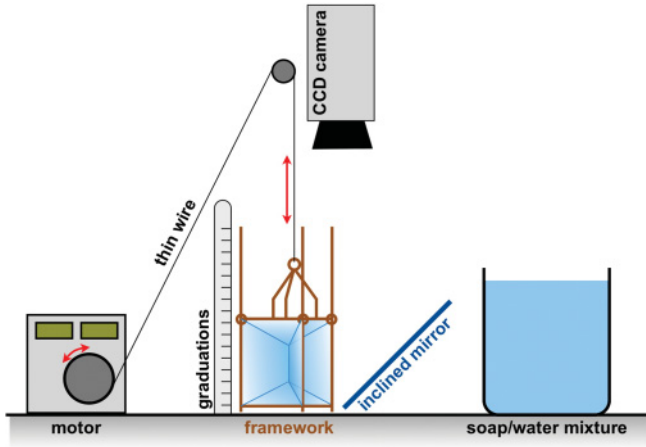


FIG. 5. (Color online) Sketch of the experimental setup. The frame is immersed into a soap and water mixture. After removing the frame from the solution, thin soap films are created. A motor can increase continuously or decrease  $h$  by using a thin wire. Above the framework, a high definition CCD camera records top and lateral images of the soap films with the help of an inclined mirror.

the free drainage. The thin films are then observed through a high resolution charge-coupled device (CCD) camera placed above the prism. An inclined mirror allows us to record lateral and top images of the film structures. The mobile part of the framework is attached to a motor through a thin wire (see Fig. 5). This motor allows us to change continuously and slowly the aspect ratio  $h = H/A$  of the prism. In the present study,  $h$  is modified step by step allowing the structure to relax before each image recording. On all images, the area  $\Delta$  of the horizontal face (configuration I<sub>curved</sub>) and the length  $L$  of the vertical Plateau border (configuration II) are determined. Those data are normalized by the edge length  $A$ , i.e.,  $\sigma = \Delta/A^2$  and  $\ell = L/A$ . Please note that the surface area  $\Delta$  is not determined through the measurement of edge  $B$  (see Fig. 1) because the face is not exactly a regular triangle but has rather round edges. The measurements are shown in Fig. 6.

Figure 6 presents the dimensionless parameters  $\sigma$  and  $\ell$  during typical experimental runs for which the prism shape ratio  $h$  either increases (triangles up) or decreases (triangles down). Numbered arrows indicate the sequence of behaviors in a typical experimental run. When the  $h$  factor increases from a low value (arrow 1), the configuration I<sub>curved</sub> remains until a critical point (arrow 2) above which configuration II is observed (arrow 3). When  $h$  decreases from a high value (arrow 4), it remains unchanged (except for the length  $\ell$  of the plateau border which decreases linearly) until a critical point is encountered (arrow 5). Below this point (arrow 6), configuration I<sub>curved</sub> is obtained.

In Fig. 6, the different trends are emphasized by thick gray lines. In both plots, a clear hysteric loop is observed. The hysteresis, emphasized by colored polygons in the figures, means that the system is trapped in local minima of the free energy. The soap films remains out of global equilibrium. The borders of the loop should correspond to instability points emphasized in Fig. 3. However, the thresholds in Fig. 6 seem to be slightly shifted by 0.03 from theoretical values predicted using Surface Evolver. These small differences

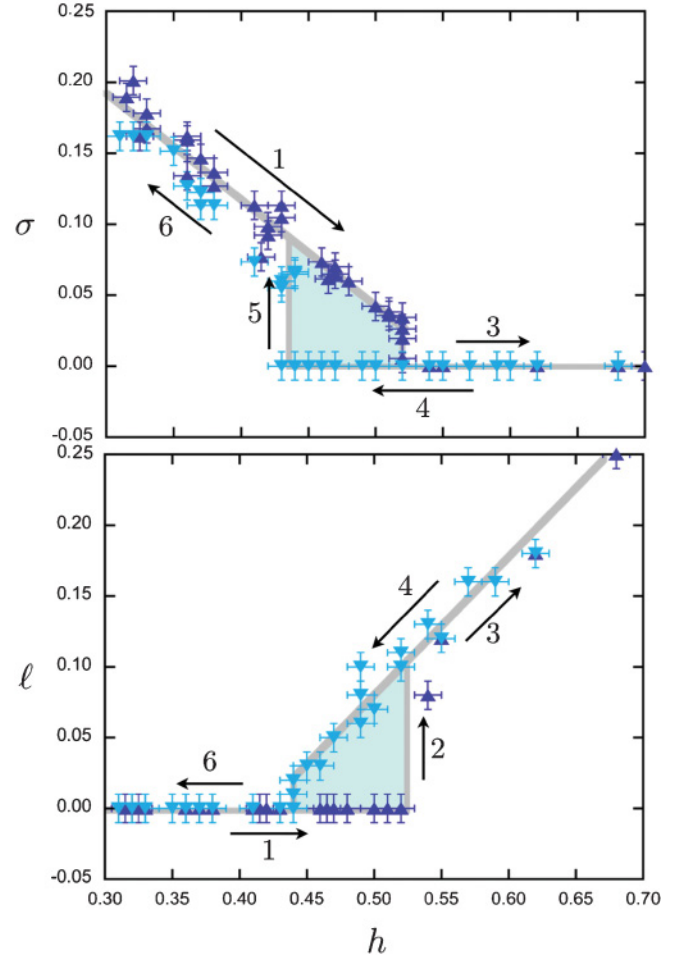


FIG. 6. (Color online) Measurements of the geometrical characteristics for configurations I and II as a function of the dimensionless parameter  $h$ . Error bars are indicated. (top) The area  $\sigma = \Delta/A^2$  of the horizontal face for configuration I. (bottom) The vertical length  $\ell = L/A$  of the Plateau border in configuration II. In both plots, the experimental data are represented by either up or down triangles for respectively increasing  $h$  and decreasing  $h$  situations. The trend of the data are emphasized by gray lines, as guides for the eye. The hysteric loop is emphasized by a filled polygon. Numbered arrows indicate the experimental sequence (see text).

between theoretical and experimental values have various possible origins: (i) The wires have a non-negligible diameter (1 mm) such that a systematic correction should be applied to data. (ii) Gravity could play a role on the liquid motion. The presence of such an additional force could have a large effect, depending on the liquid content.

When we start the experiment immediately after creating the soap films, the data for respectively increasing  $h$  and decreasing  $h$  do not collapse on the same curve, even far from the critical points. The liquid drainage has a relevant effect on our observations. In order to minimize as much as possible those effects, we wait for 30 sec of free drainage before starting the measurements. Following this procedure, we check on Fig. 6 that both  $\ell$  and  $\sigma$  data collapse when increasing and decreasing  $h$ . The liquid content should be as low as possible in order to obtain reproducible observations.

### III. DISCUSSION

Surface Evolver and similar algorithms are unable to provide information about situations out of equilibrium since they are based on some minimization search. In order to study the free energy landscape around equilibrium situations, we considered the idealized cases for which flat surfaces are only observed. They are illustrated in Fig. 1. Only configuration  $I_{\text{flat}}$  is an approximation of the experimental structure  $I_{\text{curved}}$ . Following basic geometry calculations, configuration  $I_{\text{flat}}$  has a total (dimensionless) area

$$s_{I_{\text{flat}}} = \frac{\sqrt{3}}{4}b^2 + \frac{\sqrt{3}}{2}h(1-b) + 3(1+b)\sqrt{\frac{h^2}{4} + \frac{(1-b)^2}{12}}, \quad (1)$$

which is a function of the prism height  $h$  and the length  $b = B/A$  of the triangular edge in the center of the structure. For this configuration, one has  $\sigma = \sqrt{3}b^2/4$ . It should be noted that for each fixed value  $h < 0.442$ , a minimum of the surface area can be found. For higher  $h$  values, configuration  $I_{\text{flat}}$  becomes unstable since the minimum of  $s_{I_{\text{flat}}}$  corresponds to  $b = 0$ , i.e., to a sixfold vertex. The surface area of the stable configuration  $I_{\text{flat}}$  is also shown in Fig. 3. This surface area is close to the curved configuration, meaning that the approximation is excellent. However, the instability point is much lower than for the curved configuration. When considering  $I_{\text{flat}}$  instead of  $I_{\text{curved}}$ , the interval for the coexistence between configurations I and II becomes smaller. Nevertheless, this particular configuration gives relevant information about our results, as we will see below.

The normalized surface area of configuration II is given by

$$s_{\text{II}} = \frac{\sqrt{3}}{2}(h + \ell) + 3\sqrt{\frac{1}{12} + \frac{(h - \ell)^2}{4}}, \quad (2)$$

which is a function of prism height  $h$  and vertical Plateau border length  $\ell$ . A minimum of this surface area is found for  $\ell = h - 1/\sqrt{6}$ . Avoiding the meeting of the vertices ( $\ell > 0$ ) implies that  $h > 1/\sqrt{6}$ .

Since any transition between  $I_{\text{flat}}$  and II structures implies a continuous change of  $b$  and  $\ell$ , it is possible to draw some “free energy landscape”  $s$  around both configurations by considering a hybrid horizontal axis  $(b, \ell)$  as shown in Fig. 7. The left part ( $b$  axis) corresponds to the dimensionless area of  $I_{\text{flat}}$  arrangements while the right part corresponds to double tetrahedra structures (II). Different curves [Eqs. (1) and (2) for respective parts] are presented for different  $h$  values between  $h = 0.39$  and  $h = 0.46$  by steps of 0.01. For low (respectively high)  $h$  values, the free energy landscape presents a single minimum being a type I (respectively II) configuration. In between  $h = 1/\sqrt{6}$  and  $h \approx 0.44$ , two minima are seen meaning that both configurations exist. An energy barrier separates both minima. This barrier is responsible for the metastability by assuming that any excess of elastic energy is dissipated in the system. One should also remark that the transitions defining the boundaries of the hysteric loop have different physical features. Indeed, a second order transition is observed for the disappearance of structure II while the  $I_{\text{flat}}$

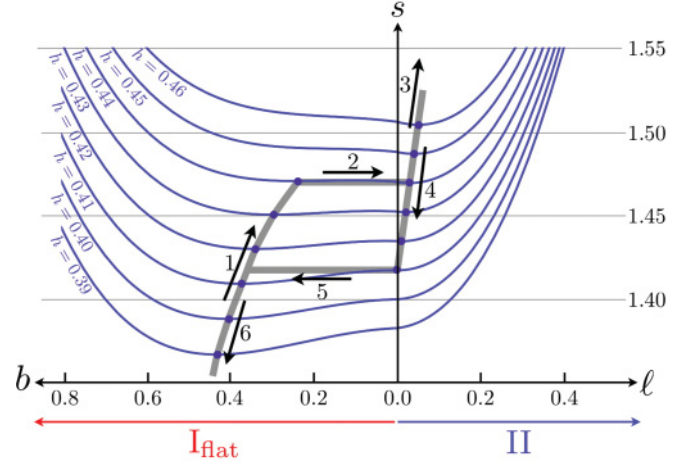


FIG. 7. (Color online) Energy landscape of both idealized configurations  $I_{\text{flat}}$  (through parameter  $b$ ) and II (through parameter  $\ell$ ) for different  $h/a$  values. The dots indicate the global and local minima for each curve. The hysteresis loop is emphasized by thick gray curves and arrows numbered according to Fig. 6.

configuration vanishes abruptly (like a first order transition) when changing  $h$ .

The coexistence of different stable soap film structures has also been evidenced for round bubbles placed between two parallel plates [9]. In such a system, hysteric loops are also found. The hysteric features reported here for an idealized system should be present in real foam structures. Indeed, foam generation [10], foam coarsening, foam rheology, and foam collapse [11] are dominated by local topological rearrangements. Recent advances [12] have indeed underlined the link between bulk and interfacial rheology and the dynamics of T1 and T3 rearrangements. One should also note that metastability implies memory effects which could play a role in foam rheology.

### IV. CONCLUSION

In summary, we proved experimentally the existence of metastability in soap film structures. We proposed a geometrical model based on idealized configurations. This model captures the physical phenomena associated with our experiments, i.e., hysteresis and abrupt transitions.

Future works concern other framework geometries, as proposed by Lovett [4]. The effect of the liquid content could be also investigated.

Finally, it should also be noted that this experiment illustrates the concept of metastability in a straightforward way. It could be used for educational purposes.

### ACKNOWLEDGMENTS

This work has been financially supported by the ESA MAP AO-99-108 entitled “Hydrodynamics of Wet Foams.” The authors thank also the support of the INANOMAT project (Grant No. IAP P6/17) of the Belgian Science Policy. The precious help of J. C. Remy for building the triangular framework is acknowledged. S.D. and G.L. were financially supported by FNRS (Brussels, Belgium).

- [1] J. A. F. Plateau, *Statique Expérimentale et Théorique des Liquides soumis aux Seules Forces Moléculaires* (Gauthier-Villars, Paris, 1873), Vols. 1 and 2.
- [2] D. Weaire and S. Hutzler, *The Physics of Foams* (Oxford University Press, New York, 2000).
- [3] D. G. T. Barrett, S. Kelly, E. J. Daly, M. J. Dolan, W. Drenckhan, D. Weaire, and S. Hutzler, *Microgravity Sci. Technol.* **20**, 17 (2008).
- [4] D. Lovett, *Phys. Educ.* **14**, 40 (1979).
- [5] D. Weaire, M. F. Vaz, P. I. C. Teixeira, and M. A. Fortes, *Soft Matter* **3**, 47 (2007).
- [6] S. Hutzler, D. Weaire, S. J. Cox, A. van der Net, and E. Janiaud, *Europhys. Lett.* **77**, 28002 (2007).
- [7] S. Hutzler, M. Saadatfar, A. van der Net, D. Weaire, and S. J. Cox, *Colloids Surf. A* **323**, 123 (2008).
- [8] K. A. Brakke, *Exp. Math.* **1**, 141 (1992).
- [9] S. Bohn, *Eur. Phys. J. E* **11**, 177 (2003).
- [10] H. Caps, N. Vandewalle, and G. Broze, *Phys. Rev. E* **73**, 065301 (2006).
- [11] N. Vandewalle, J. F. Lentz, S. Dorbolo, and F. Brisbois, *Phys. Rev. Lett.* **86**, 179 (2001).
- [12] A.-L. Biance, S. Cohen-Addad, and R. Höhler, *Soft Matter* **5**, 4672 (2009).